Journal of
Nanoscience and Nanotechnology
Vol. 5, 1792–1800, 2005

RESEARCH ARTICLE

Photolithographic Patterning of Dendrimer Monolayers and Pattern-Selective Adsorption of Linear Macromolecules

Tomoko Yamazaki,[1] Toyoko Imae,[1,2,*] Hiroyuki Sugimura,[3] Nagahiro Saito,[4] Kazuyuki Hayashi,[5] and Osamu Takai[6]

[1] Graduate School of Science and [2] Research Center for Materials Science, Nagoya University, Chikusa, Nagoya 464-8602, Japan
[3] Graduate School of Engineering, Kyoto University, Sakyo-ku, Kyoto 606-8501, Japan
[4] Graduate School of Engineering, Nagoya University, Chikusa, Nagoya 464-8603, Japan
[5] Asahi Glass Co., Ltd., 1-12-1 Yurakucho, Chiyoda-ku, Tokyo 100-8405, Japan
[6] EcoTopia Science Institute, Nagoya University, Chikusa, Nagoya 464-8603, Japan

Alkyl groups of *n*-octadecyltrimethoxysilane (ODS) in a self-assembled monolayer on a silicon substrate were oxidized to carboxyl groups by partial irradiation of vacuum ultra-violet light under the photomask, producing a COOH/ODS line pattern. After active esterification of carboxyl groups, two kinds of amine-terminated dendrimers, poly(propyleneimine) and poly(amido amine) (PAMAM) dendrimers, were immobilized on a COOH line through amide-bond so that photolithographic dendrimer/ODS pattern was finally fabricated. Preparation was certified by atomic force microscopy (AFM) and surface-enhanced infrared absorption spectroscopy at transmission mode. Adsorption of linear macromolecules was examined on PAMAM dendrimer/ODS pattern. After adsorption of poly-*L*-glutamic acid (PGA) at a pH below α-helix—random coil transition, rod-shape texture was observed only on the dendrimer line in an AFM image. This texture is an aggregate of α-helical PGA. Sodium hyaluronate and DNA were also adsorbed selectively on the dendrimer line, keeping the line profile, although characteristic textures were not observed.

Keywords: Photolithographic Pattering, Photolithography, Dendrimer, Poly(propyleneimine) Dendrimer, Poly(amido Amine) Dendrimer, Self-Assembled Monolayer, *n*-Octadecyltrimethoxysilane, Atomic Force Microscopy, Surface-Enhanced Infrared Absorption Spectroscopy, Poly-*l*-glutamic acid, Sodium hyaluronate, DNA, Linear Macromolecule.

1. INTRODUCTION

Rigorous control at molecular scale in the chemical property and structure of thin films has been demanded in the last decade, since the functionality and application of the thin films can be affected even by small amount of molecules. As one of effective constituents of functional films, dendrimers with highly-fabricated chemical structure, functional terminal groups in periphery, and nanocavities in internal have been used,[1–3] since the dendrimers enhance the advantage of conventional polymer. There have been many reports regarding thin films of dendrimers which are expected the capability as chemical sensors,[4–6] electronic or optical devices,[7,8] and templates for nanoparticles[9,10] by using specific chemical species. On the immobilization of dendrimer to the substrate, covalent-bond avoids the removal of dendrimer from the substrate and increases the chemical stability of the films against the variation of conditions as pH, temperature, and pressure, in comparison with electrostatic-binding on acid/base self-assembling method.[11–13] It has been reported that amine-terminated dendrimer was bound on

*Author to whom correspondence should be addressed.

 1533-4880/2005/5/1792/009 doi:10.1166/jnn.2005.434

the substrate, which was converted into acid anhydride by acyl chloride.[14,15]

On the other hand, there have been some reports on the preparation of patterned thin films of dendrimer using patterning methods such as micro-contact printing[16,17] and scanning probe lithography,[18] although the interaction between dendrimer and substrate remains in electrostatic-binding, which is less stable than covalent-bond. Among various patterning methods, photolithography is most practical and industrially applicable, since it can transfer a pattern on photomask to a substrate by single exposure.[19,20] According to this method, alkyl groups of *n*-octadecyltrimethoxysilane (ODS) in self-assembled monolayer (SAM) was converted to carboxyl groups during the irradiation of vacuum ultra-violet (UV) light.[21,22] Consequently, partial irradiation to ODS SAM under the photomask provided the pattern that consists of carboxyl groups and ODS (COOH/ODS pattern). Thus, a molecule having amine groups can react with carboxyl groups on a COOH line.

In this work, photolithography and immobilization techniques were combined to create a novel patterned film of dendrimer. By using amide-coupling reagents, amine-terminated dendrimer was covalently bound by amide-bond to the carboxyl-terminated line on the patterned substrate. Each process on the formation of the patterned film was verified by atomic force microscopy (AFM) and surface-enhanced infrared absorption (SEIRA) spectroscopy at transmission mode.[23,24] Furthermore, effects of irradiation time of vacuum UV light and dendrimer concentration on patterning were investigated.

Patterned film consisting of dendrimer is expected as an efficient interfacial reaction matrix, since it would have advantages such as the high reactivity of terminal groups on the dendrimer line and the selectivity of binding sites on the dendrimer/non-dendrimer pattern. Kern and coworkers[25,26] have reported that dendrimer pattern formed by the micro-contact printing method served as a template for spatially selective electroless deposition of metal. On the other hand, dendrimer SAM was used as a DNA detector[27] and a biochemical sensor based on protein–ligand interaction.[28,29] In those cases, terminal groups of dendrimer were modified by chemical species which has an affinity to a target.

By contrast, the simple system utilizing direct interaction with dendrimer also plays an important role as mimic biomembrane including host-guest system,[30–34] since dendrimer itself can act as a host molecule without further modification. Interactions between dendrimers and biomacromolecules or linear polymers, which were mainly electrostatic and hydrogen bonds, have been studied in solutions or at interface.[35–40] Based on these studies, in the present work, adsorption behaviors of sodium poly-*L*-glutamate (NaPGA), sodium hyaluronate (NaHA) and DNA were examined on dendrimer/ODS pattern, and surface morphology was observed by AFM.

2. EXPERIMENTAL DETAILS

2.1. Materials

ODS was a product from Tokyo Kasei Organic Chemicals. A 10 wt% methanol solution of fourth generation (G4) poly(amido amine) (PAMAM) dendrimer, fifth generation (G5) poly(propyleneimine) (PPI) dendrimer, 1-ethyl-3-(3-dimethylaminopropyl)-carbodiimide hydrochloride (EDC) and *N*-hydroxy succinimide (NHS) were purchased from Aldrich. NaPGA was synthesized by polymerization of *L*-glutamic acid. NaHA (m.w. $\sim 1.2 \times 10^6$ Da) was donated from Shiseido Co. Ltd. DNA (sodium salt from salmon testes), ethanol, methanol, acetone and hydrochloric acid were obtained from Wako Pure Chemical Industries. Distilled, deionized water (MilliQ water) was used throughout the work. The silicon substrate (Shin-etsu Handoutai, N-type(100) wafer) was cleaned by ultrasonication in acetone, ethanol and water, and photochemically by exposure for 20 min in vacuum UV light generated from an excimer lamp (Ushio Electric UER20-172V, $\lambda = 172$ nm with a power density of 10 mW/cm^2), where the direct photoexcitation and the produced active oxygen by vacuum UV light irradiation decomposed organic contaminants.[41–43]

2.2. Measurements

AFM observation at contact mode was performed on a Seiko Instruments SPA-300HV + SPI-3800N microscope using a gold-coated silicon tip in large scale scanning ($>20 \times 20\ \mu$m^2) and a Digital Instruments Nanoscope III microscope using a crystalline silicon tip in small scale scanning ($<10 \times 10\ \mu$m^2). A clean silicon wafer was used as a substrate.

SEIRA spectroscopic measurement at transmission mode was carried out on a Bio-Rad FTS 575C FT-IR spectrometer equipped with a liquid nitrogen-cooled cryogenic mercury cadmium telluride (MCT) detector. Gold island film that enhances the intensity of an infrared absorption band was deposited on clean silicon substrates, as described elsewhere.[44,45] All the measurements were performed at room temperature. Although the interaction of ODS to gold islands is weaker than that to silicon wafer, the qualitative analysis from SEIRAS is possible and comparable to AFM results.

3. RESULTS AND DISCUSSION

3.1. Formation of Dendrimer/ODS Patterned Film

ODS SAM was prepared on silicon (or gold deposited silicon) substrates by the chemical vapor deposition method.[41,46] ODS gas evaporated at 423 K from liquid was adsorbed for 3 h on the substrates in a sealed vessel so as to form SAM. ODS SAM was exposed through a photomask in vacuum UV light in the presence of oxygen.[21,22,47,48] The irradiation was carried out at

RESEARCH ARTICLE

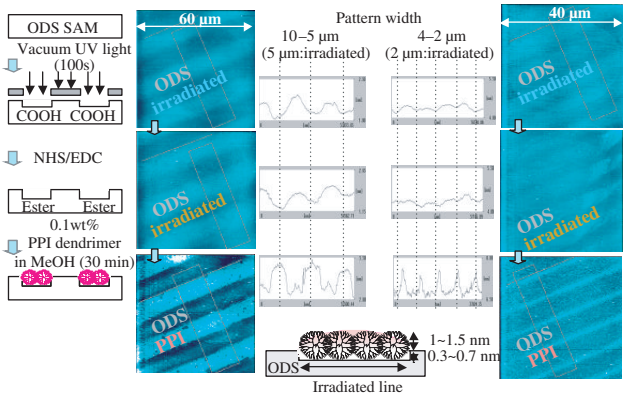

Fig. 1. AFM images at each reaction step on PPI dendrimer/ODS pattern formation. The size of section analysis is 1.5 nm and 54 μm (longitudinal and abscissa axes) for 10–5 μm pattern and 1.5 nm and 37 μm (longitudinal and abscissa axes) for 4–2 μm pattern.

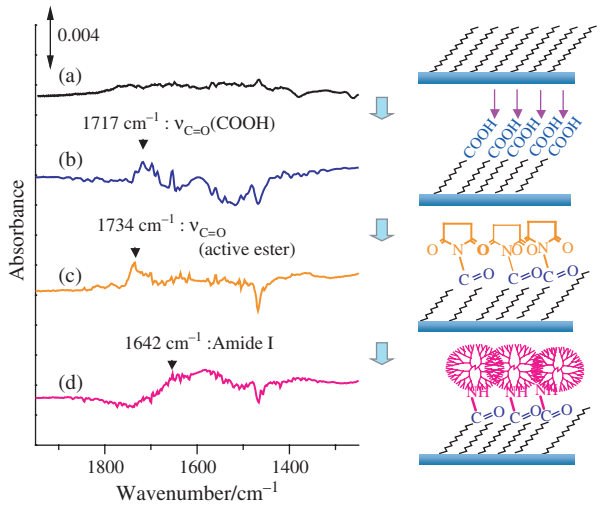

Fig. 2. SEIRA spectra at each reaction step on PPI dendrimer/ODS pattern formation (a) ODS SAM (b) vacuum UV light irradiation (100 s) (c) active esterification (d) PPI dendrimer immobilization (0.1 wt%, 30 min).

atmosphere pressure and with a proximate gap of <10 nm between the substrate and photomask. ODS SAM was gradually oxidized during the exposure of ~100 s in vacuum UV light, partially converting alkyl groups of ODS into carboxyl groups, although it was all decomposed after exposure for more than 200 s.[21, 22] Formation of carboxyl groups was confirmed by water contact angle (Kyowa Interface Science CA-X150) and film thickness from ellipsometry (Philips Japan PZ2000). The COOH/ODS patterned substrate obtained was immersed into a freshly prepared aqueous solution of NHS/EDC (0.013 M each) to convert the carboxyl groups into active ester groups.[49] After rinsed by water, the substrate was reacted with dendrimer in methanol.

The observation of AFM images was carried out at each step of the reaction process on the formation of PPI dendrimer/ODS pattern. Figure 1 shows two cases on the preparation using photomasks of different line widths (10–5 and 4–2 μm). Images are composed of lines, that is, irradiated and unirradiated regions, whose widths are 5 (or 2) and 10 (or 4) μm, respectively. After the formation of carboxyl groups by vacuum UV light irradiation for 100 s, height lowering from unirradiated region was 0.3 ~ 0.7 nm. This height difference was unchanged even after the active esterification by NHS/EDC. After the substrate was immersed into a 0.1 wt% methanol solution of PPI dendrimer, the irradiated lines in the patterned substrates became higher than the unirradiated regions. Moreover, surface roughness of the irradiated line increased to 0.4 nm, while that of the unirradiated region did not vary from ~0.2 nm, which is almost equivalent to the roughness of original ODS SAM. It was supposed that the inversion of height and the increase of surface roughness occurred due to the binding of PPI dendrimers on the irradiated lines. It was also confirmed that PPI dendrimers did not adsorb on ODS SAM. These results suggest that PPI dendrimer was pattern-selectively immobilized. It was evaluated from the observation in small scale scanning that height difference of the PPI dendrimer line from the ODS region was 1 ~ 1.5 nm. Then the total increase in the irradiated line after the reaction with PPI dendrimer can be estimated to 1 ~ 2 nm. This value is smaller than the calculated diameter (3 nm) of spherical G5 PPI dendrimer.[50] Thus, it is assumed that PPI dendrimer forms a monolayer but is flattened (see Fig. 1).

In order to confirm spectroscopically the reaction, transmission SEIRA spectroscopic investigation was carried out for films on a gold-deposited silicon substrate. In this investigation, a bare gold-deposited silicon substrate without film was used as a background. As seen in Figure 2, SEIRA bands at each reaction step appeared at the similar positions to those on homogeneous dendrimer SAM (data are not shown). No strong or significant bands of ODS SAM were observed in the region of 1800 ~ 1400 cm^{-1}. However, after vacuum UV irradiation, a C=O stretching band was visible at 1717 cm^{-1}, indicating the formation of carboxyl group on ODS SAM. A band at 1734 cm^{-1}, appeared instead of 1717 cm^{-1} after active esterification by NHS and EDC, was assigned to a C=O stretching vibration mode of active ester. Finally, amide I band at 1642 cm^{-1} was observed but a band at 1734 cm^{-1} disappeared after immersing the substrate into a PPI dendrimer solution. Thus, amide-linkage was formed between carboxyl group in irradiated line and terminal amine group of dendrimer. This proves that dendrimer is covalently linked to the ODS patterned film.

The condition on the preparation of PAMAM dendrimer/ODS patterned film was examined. As shown in Figure 3, although short time irradiation (<100 s) would minimize the blur around the edge of pattern, it was not enough to form carboxyl groups, and PAMAM dendrimer was hardly found on the irradiated line in the substrate. Then the irradiation time of 100 s was determined to

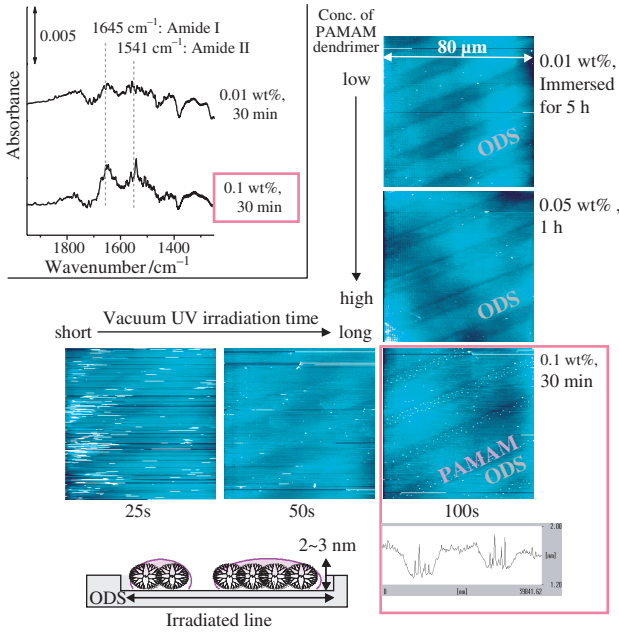

Fig. 3. Condition of PAMAM dendrimer/ODS pattern formation (vacuum UV light irradiation time, dendrimer concentration, immersing time). Insert is SEIRA spectra of PAMAM dendrimer/ODS patterned film. The size of section analysis is 0.8 nm and 40 μm (longitudinal and abscissa axes).

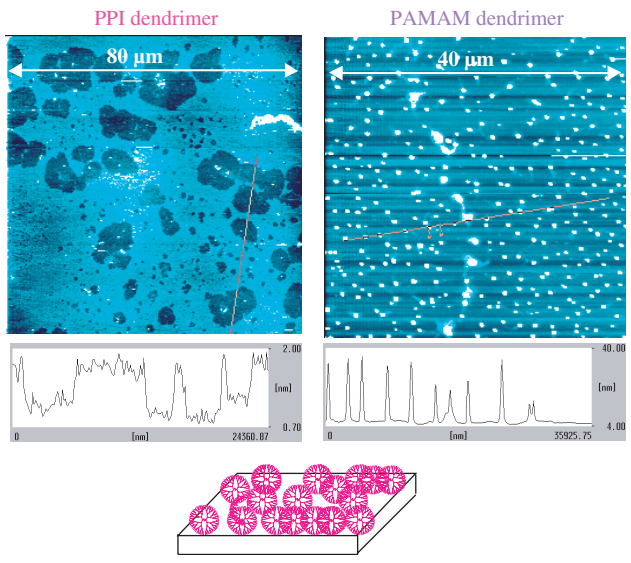

Fig. 4. AFM images of dendrimer films on ODS SAM prepared without photomask (100 s irradiation, 0.1 wt% dendrimer concentration, 30 min immersion). The size of section analysis is 1.3 nm and 24 μm (longitudinal and abscissa axes) for PPI dendrimer and 16 nm and 36 μm (longitudinal and abscissa axes) for PAMAM dendrimer.

be adequate. At a PAMAM dendrimer concentration of 0.01 wt%, the immersing time of neither 30 min nor 5 h was enough to observe dendrimer (data is not shown in the case of 30 min). Situation was same even for 1 h reaction in a 0.05 wt% dendrimer solution. When immersed for 30 min in a 0.1 wt% dendrimer solution, the existence of some globular particles was ensured on the irradiated line. Therefore, this condition seems proper to prepare PAMAM dendrimer/ODS pattern. An effect of the concentration of a dendrimer solution immersed was investigated by SEIRA spectroscopy. While amide I and II bands of PAMAM dendrimer were very weak at a 0.01 wt% solution, obvious bands appeared at a 0.1 wt% solution (see Fig. 3). Thus, the concentration of PAMAM dendrimer was fixed at 0.1 wt% in the experiment from now on. An AFM image of PAMAM dendrimer/ODS pattern at small scale scanning indicated that the dimension of globular particles in the irradiated line was $2 \sim 3$ nm in height and more than 100 nm in width. Considering a size of spherical G4 PAMAM dendrimer (calculated diameter = 4.5 nm[51]), the particles were supposed to be aggregates of flattened PAMAM dendrimers.

As comparison, uniform dendrimer film was prepared by vacuum UV light irradiation (100 s) without photomask on whole surface of ODS SAM. Figure 4 compares AFM images of dendrimer films on ODS SAM fabricated on silicon substrates using PAMAM and PPI dendrimers (a 0.1 wt% methanol solution). The sectional defects can be observed in an AFM image of PPI dendrimer film, as well as in dendrimer line of the PPI dendrimer/ODS pattern. These defects would occur owing to inhomogeneous vacuum UV light irradiation that leads to the lack of carboxyl groups. The surface of the PPI dendrimer film was fairly homogeneous and flat in the region except the defects. The height difference of 1 nm in the film image was close to the total increase in PPI dendrimer/ODS pattern. On the other hand, in PAMAM dendrimer film, most of the surface consists of globular particles that are similar to the texture in the PAMAM dendrimer line of the dendrimer/ODS pattern. Moreover, larger aggregates were also observed. Many amide and amine groups in a PAMAM dendrimer strongly interact by intermolecular hydrogen bonding, which results in high aggregation between dendrimers. In addition to inhomogeneous vacuum UV light irradiation, such aggregation would bring a negative effect on the formation of smooth PAMAM dendrimer film, different from the case of a PPI dendrimer that has no amide bonds. Nagaoka and Imae[12] confirmed the difference of adsorption structures between PPI and PAMAM dendrimers on the adsorption from aqueous solutions to carboxyl-terminated SAM. In the present work, amount of carboxyl group on the substrate evaluated from SEIRA spectra was not large. In addition, the solubility of dendrimers in methanol and the binding structure of dendrimers on substrate would cause different behaviors between PPI and PAMAM dendrimers.

3.2. Pattern-Selective Adsorption of Macromolecules

Sodium poly-*L*-glutamate (NaPGA): Complexiation of NaPGA with PAMAM dendrimer has been investigated in aqueous solutions[36–39] and on dendrimer SAM.[49] In the

present work, adsorption of PGA was examined on dendrimer/ODS pattern and compared with the case on dendrimer SAM. Four types of substrates (ODS SAM patterned with PAMAM dendrimer, PAMAM dendrimer SAM, ODS SAM, and mica) were immersed into an aqueous NaPGA solution (0.02 wt%) at pH 4.26, which was adjusted by adding an aqueous HCl solution. After the reaction for 30 min, they were rinsed with water at pH 4.26. These optimum conditions for the adsorption were previously determined.[49] AFM images in Figure 5 show surface observation of the before-and-after adsorption of PGA on PAMAM dendrimer/ODS pattern. The average height increase of dendrimer line calculated from height difference in cross sectional analysis was 10 ~ 20 nm.

Before the reaction with PGA, no significant textures were seen, except some defects, in an AFM image of dendrimer line (see images at high magnification, 5 × 5 μm, in Fig. 5). However, after reacting with PGA, rod-shape textures appeared only on PAMAM dendrimer line (Figs. 5 and 6). Height difference of these textures from the surface

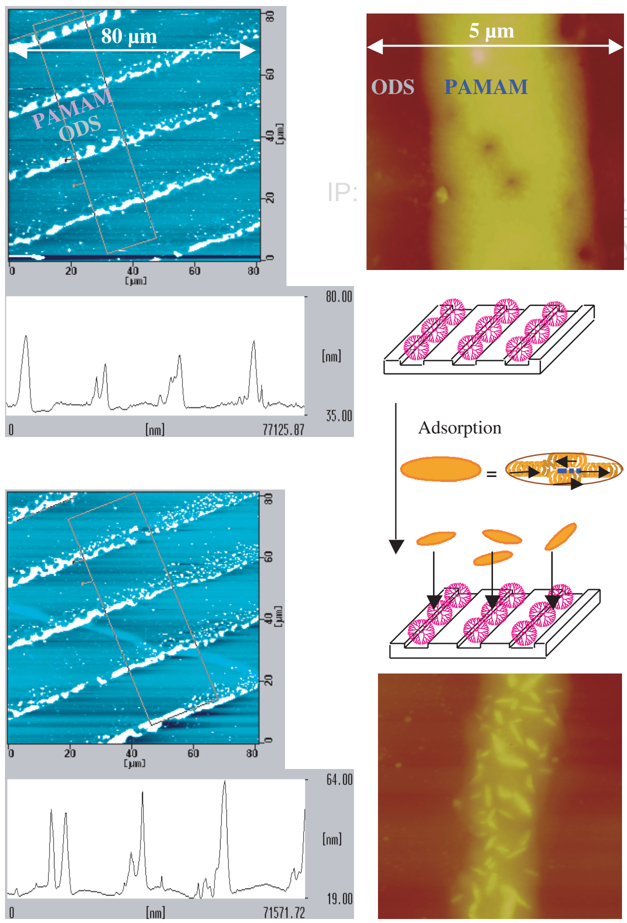

Fig. 5. AFM images of before-and-after adsorption of PGA on PAMAM dendrimer/ODS pattern of 10–5 μm pattern width (5 μm:irradiated). PGA adsorption (0.02 wt% dendrimer concentration, pH 4.26, 30 min immersion). The size of section analysis is 45 nm and 77 μm (longitudinal and abscissa axes) for before adsorption and 45 nm and 72 μm (longitudinal and abscissa axes) for after adsorption.

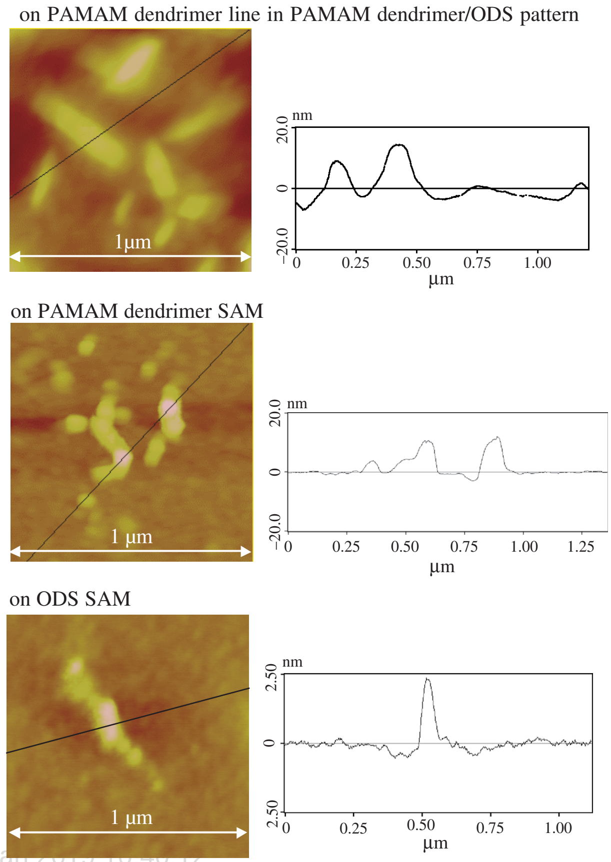

Fig. 6. AFM images of PGA adsorbed on dendrimer line in PAMAM dendrimer/ODS pattern, on PAMAM dendrimer SAM, and on ODS SAM. (0.02 wt% dendrimer concentration, pH 4.26, 30 min immersion).

of dendrimer line was 15 ~ 20 nm in concurrence with the increase in large scale AFM described above. Therefore, these textures were supposed to be composed of PGA. Adsorption of PGA was also investigated on homogeneous PAMAM dendrimer SAM fabricated on silicon substrate. As was expected, similar AFM texture to that on the dendrimer line of dendrimer/ODS pattern was observed on the dendrimer SAM (Fig. 6).

It is suggested that PGA on the PAMAM dendrimer takes α-helical structure, because the adsorption reaction was carried out at pH 4.26 below α-helix—random coil transition pH of PGA. The formation of α-helical structure of PGA was determined from amide I and II bands of infrared absorption spectra on homogeneous PAMAM dendrimer SAM at acidic pH.[49] Since rods in AFM images (Fig. 6) have a width of 50 ~ 150 nm and a length of 100 ~ 250 nm, they would be aggregates but not a single PGA molecule. In an α-helical PGA, hydrogen-bond between C=O and N—H is parallel to helical axis, yielding permanent dipole moment along helical axis.[52, 53] It is supposed that PGA molecules aggregate by dipole–dipole interaction of PGA and by intermolecular hydrogen-bonding between COOH groups of side chains, resulting in the formation of bundles by side-by-side or head-to-tail arrangement of

PGA molecules. Proposal model for aggregates is shown in Figure 5. Binding interaction on the PAMAM dendrimer line in dendrimer/ODS pattern is hydrogen-bond between carboxylic acid group of PGA and terminal protonated amine group and/or amide group of PAMAM dendrimer. Similar interaction was reported for PGA adsorption on PAMAM dendrimer SAM.[49]

Adsorption on the other substrates, that is, ODS SAM and freshly cleaved mica was investigated for comparison. PGA adsorbed only slightly on ODS SAM (Fig. 6), and the adsorption was far less than that on dendrimer SAM. This would occur due to less solubility of PGA in water at acidic pH, because PGA is protonated at lower pH than pKa (∼4.8) of NaPGA.[36, 38] On the other hand, no rods were observed on the ODS region in PAMAM dendrimer/ODS pattern (Fig. 5). It is presumed that at the adsorption on PAMAM dendrimer/ODS pattern, the interaction of PGA with PAMAM dendrimer took priority of that with ODS SAM. This means that PGA recognized PAMAM dendrimer and adsorbed selectively on it.

In contrast, the surface of mica after the procedure of PGA adsorption was almost flat with height difference within 0.2 nm (data is not shown). Since many carboxylic acid groups in PGA can bind to hydroxy-terminated mica surface via hydrogen-bond, immersing time (30 min) would be enough to attain the adsorption equilibrium. Moreover, a layer with thickness less than 0.5 nm was shown in an AFM image of a deposited film on mica that was prepared by dropping an aliquot of PGA solution (data is not shown). Both cases did not show rod-like texture of aggregates unlike the surface of PAMAM dendrimer. Thus, it is assumed that the interaction between PGA and substrate affects on the formation of the attractive texture such as rod.

Sodium Hyaluronate (NaHA): It was reported that PAMAM dendrimers adsorb on NaHA chains in an aqueous solution, till NaHA chains are saturated by adsorbed dendrimers.[35] It was assumed that hydrogen-bond between hydroxyl groups of HA and amine and/or amide groups of PAMAM dendrimer became dominant besides electrostatic interaction between carboxylate ions of NaHA and protonated terminal amines of PAMAM dendrimer. The substrates (PAMAM dendrimer/ODS pattern, PAMAM dendrimer SAM, ODS SAM and mica) were immersed into an aqueous NaHA solution (0.04 wt%) at pH 3.82 and rinsed with water at pH 3.82 after the reaction for 30 min.

It was indicated from AFM images and cross sectional analyses that the height difference increased after the adsorption of NaHA on the PAMAM dendrimer line in dendrimer/ODS pattern (Fig. 7). This change was seen more clearly in small scale scanning. Height difference between the PAMAM dendrimer line and the ODS region was about 3.2 and 7.3 nm before and after the adsorption, respectively. Then the total increase was about 4 nm.

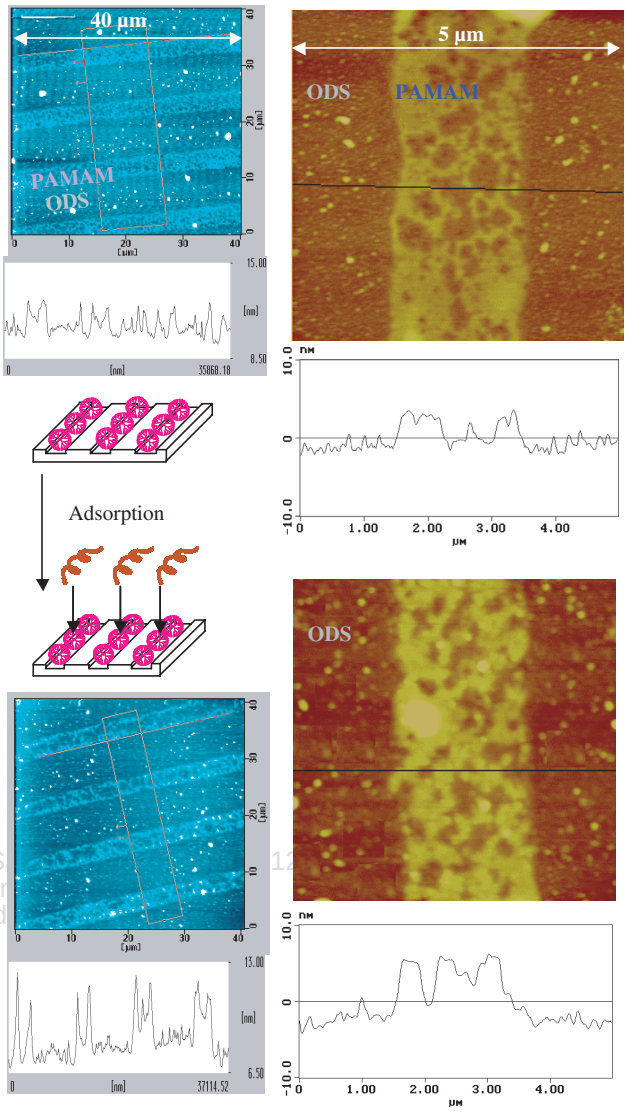

Fig. 7. AFM images of before-and-after adsorption of NaHA on PAMAM dendrimer/ODS pattern of 4–2 μm pattern width (2 μm:irradiated). NaHA adsorption (0.04 wt% dendrimer concentration, pH 3.82, 30 min immersion). The size of section analysis for large scale AFM is 7.5 nm and 36 μm (longitudinal and abscissa axes) for before adsorption and 7.5 nm and 36 μm (longitudinal and abscissa axes) for after adsorption.

To confirm that this increase occurred due to the adsorption of NaHA, AFM images of NaHA-adsorbed mica and NaHA-deposited mica were taken. On adsorption process, NaHA formed the adsorbed domains with diameter of about 150 nm whose height difference was about 3 nm (Fig. 8). On the other hand, an AFM image of NaHA-deposited mica displayed a layer of ∼3 nm height with the circular defects (Fig. 8). These heights would correspond to the thickness of NaHA film and is close to the total height increase of PAMAM dendrimer line in dendrimer/ODS pattern after the NaHA adsorption. In addition, NaHA did not adsorb on ODS SAM (Fig. 8). It is not surprised that hydrophilic charged NaHA prefers to

RESEARCH ARTICLE

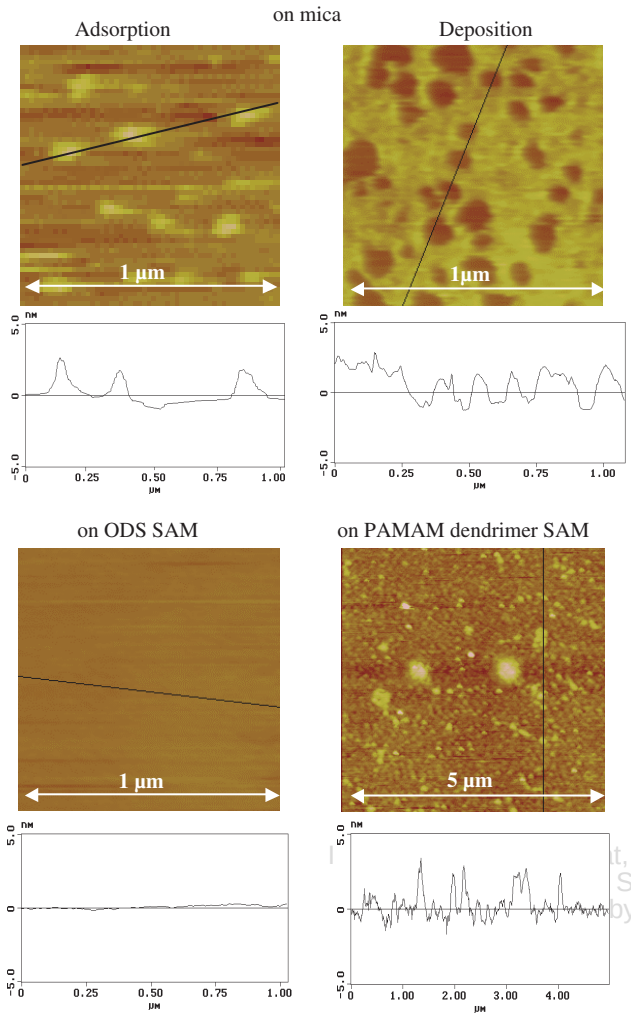

Fig. 8. AFM images of NaHA adsorbed on mica, ODS SAM and PAMAM dendrimer SAM and NaHA deposited on mica. (0.04 wt% dendrimer concentration, pH 3.82, 30 min immersion).

exist in a solution rather than interacts with the hydrophobic substrate. Thus, it is assumed that NaHA adsorbs selectively on the PAMAM dendrimer line, which results in the increase of height difference.

Adsorption of NaHA on the PAMAM dendrimer SAM was also examined. The morphology of circular domain structure was observed after the adsorption of NaHA on the PAMAM dendrimer SAM (Fig. 8). The domains had a constant height difference of about 2 nm. Considering that the height of PAMAM dendrimer line increased in whole area due to the adsorption of NaHA, an image in Figure 8 is supposed to be the surface of NaHA-covering PAMAM dendrimer SAM. The domains, having a width of 100 ~ 150 nm and a height difference of 2 ~ 3 nm, most probably resulted from the interaction of NaHA with PAMAM dendrimer, which may well contribute to the formation of complex on the surface. Larger domains, which were rarely seen, would be the accumulation of aggregates of NaHA. Some carboxyl groups of NaHA are negatively charged, because the pH of NaHA solution examined is higher than pKa (~3). Then it is assumed that the adsorption occurred mainly by the electrostatic interaction between COO^- of NaHA and NH_3^+ of PAMAM dendrimer. On the other hand, the coexistence of carboxylic acid group is also possible. This neutral carboxyl group may help the aggregation of NaHA and also leads the adsorption on dendrimer surface by hydrogen bond with NH_3^+, tertiary amine and/or amide groups of PAMAM dendrimer. Thus, NaHA at pH 3.82, which has both neutral and negatively charged carboxyl groups, is stabilized by the adsorption on dendrimer surface rather than dissolved in a solution.

DNA: Complexation of DNA with PAMAM dendrimers in aqueous solutions has been investigated at different mixing ratios of dendrimer and DNA.[40] While DNA maintained the stretched structure at lower mixing ratios, complexes at high mixing ratios were globular microgels. It is suggested that DNA and dendrimer are mainly associated with two types of interactions, electrostatic interaction between POO^- of DNA and NH_3^+ of PAMAM dendrimer (pH 2 ~ 9), and hydrogen-bond between P=O and NH_3^+ (pH < 2). An aqueous DNA solution (0.02 wt%) at pH 4.15 was prepared, and substrates (PAMAM dendrimer/ODS pattern, PAMAM dendrimer SAM, ODS SAM and mica) were immersed into this solution. After the reaction for 30 min, they were rinsed with water at pH 4.15.

AFM images in Figure 9 show the surface observation of the before-and-after adsorption of DNA on PAMAM dendrimer/ODS pattern. The dendrimer line heightened, after the adsorption of DNA, with keeping the line profile. The height differences from ODS region before and after the adsorption were about 2.9 and 8.8 nm, respectively. Consequently, the total increase due to the adsorption was about 6 nm. However, the value of 6 nm is too thick to presume to be a single DNA chain, if consider the calculated width of DNA (about 2 nm for a double-stranded DNA).

On the adsorption of DNA on PAMAM dendrimer SAM, an AFM image of PAMAM dendrimer SAM before adsorption indicated rather uniform surface without any defects (data is not shown). The surface of SAM after the reaction seemed rougher in whole region than before, which suggests the adsorption of DNA (data is not shown). Similar tendency was also seen on the PAMAM dendrimer/ODS pattern (Fig. 9). However, it was difficult to distinguish a single DNA chain from the surface of PAMAM dendrimer SAM due to the limit of resolution in this scanning scale. Probably aggregates of DNA molecules raised the roughness of the SAM. It may be noted that large fiber-like textures were observed on PAMAM dendrimer SAM, as seen in Figure 10. The height of fiber was about 5.8 nm. Since this value is close to the estimated thickness of DNA aggregates on the

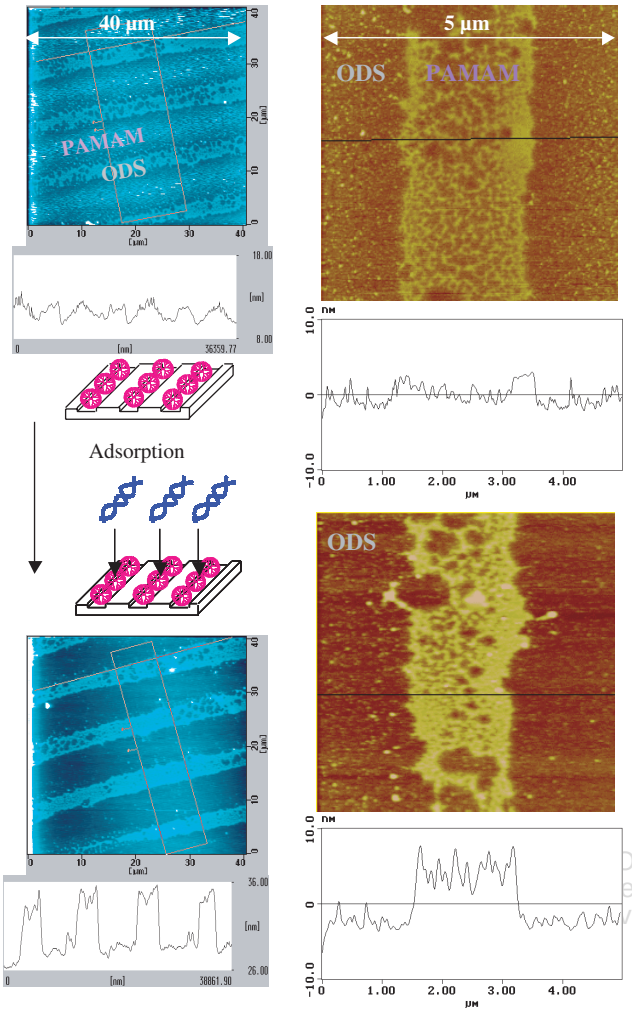

Fig. 9. AFM images of before-and-after adsorption of DNA on PAMAM dendrimer/ODS pattern of 4–2 μm pattern width (2 μm:irradiated). DNA adsorption (0.02 wt% dendrimer concentration, pH 4.15, 30 min immersion). The size of section analysis for large scale AFM is 10 nm and 36 μm (longitudinal and abscissa axes) for before adsorption and 10 nm and 39 μm (longitudinal and abscissa axes) for after adsorption.

dendrimer/ODS pattern, the aggregates in DNA adsorption layer could be fiber-like structures. Fibrous DNA also adsorbed on ODS SAM, probably due to hydrophobic interaction of ODS with partly neutralized DNA (Fig. 10). However, the interaction would be weak, because the DNA aggregates was frequently moved by an AFM probe during scanning. Thus, the interaction of DNA with PAMAM dendrimer SAM was prior to that with ODS SAM, which resulted in the selective adsorption of DNA on the PAMAM dendrimer line in dendrimer/ODS pattern. Adsorption of DNA on dendrimer at pH ~4 would occur mostly by the electrostatic interaction between POO^- of DNA and NH_3^+ of PAMAM dendrimer. Charged DNA prefers to interact with dendrimer because of electrostatic repulsion between DNAs, which supposes to give a uniform adsorption on PAMAM dendrimer.

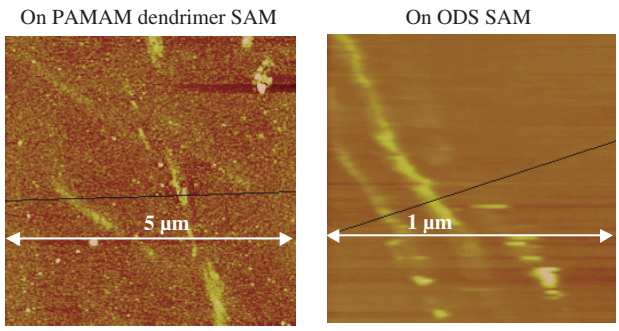

Fig. 10. AFM images of DNA on PAMAM dendrimer SAM and ODS SAM. DNA adsorption (0.02 wt% dendrimer concentration, pH 4.15, 30 min immersion).

4. CONCLUSIONS

In the present work, the formation of photolithographic dendrimer/ODS pattern was investigated by immobilization of PPI and PAMAM dendrimers via amide-bond onto COOH/ODS pattern formed by vacuum UV light irradiation to ODS SAM. On the preparation of COOH/ODS pattern, the preferable irradiation time of vacuum UV light was 100 s to form sufficient carboxyl groups. On the process of dendrimer/ODS pattern formation, SEIRA spectroscopic results confirmed the amide-bonding of amine groups of dendrimer with COOH surface. AFM observation showed that PPI and PAMAM dendrimers existed selectively on the COOH region, forming a monolayer. Owing to the intermolecular hydrogen-bonding, PAMAM dendrimer tended to aggregate on the dendrimer line.

Adsorption of linear macromolecules was examined on PAMAM dendrimer/ODS pattern. PGA formed rod-shape texture only on PAMAM dendrimer line. Rod was considered the bundle of α-helical PGA due to the dipole–dipole interaction of PGA molecules and the intermolecular hydrogen-bonding between carboxyl groups in the side chains. In the case of NaHA and DNA, the increase of the height difference on AFM images after the adsorption reaction suggested selective adsorption on the PAMAM dendrimer line, although characteristic textures like rod were not observed. The increase occurred in whole region of the dendrimer line, different from the case of PGA. This difference may correlate with the difference in major interaction between linear macromolecules and PAMAM dendrimer; that is, electrostatic interaction in the case of NaHA and DNA and hydrogen-bond in PGA.

The dendrimer monolayer films are valuable as a sensor of selective molecular recognition because of multifunctional characters of dendrimer like large number of functional terminal groups on its periphery, which were used for the adsorption of linear macromolecules. If the films are patterned, the applications of such films will extend: When non-reactive pattern in the present work is modified to functional group different from dendrimer, the patterned films will take on multiple pattern-selective functionalities for mixed systems.

RESEARCH ARTICLE

References and Notes

1. D. A. Tomalia, A. M. Naylor, and W. A. Goddard, *Angew. Chem. Int. Ed. Engl.* 29, 138 (**1990**).
2. C. J. Hawker and J. M. J. Fréchet, *J. Am. Chem. Soc.* 112, 7632 (**1990**).
3. J. M. J. Fréchet, *Science* 263, 1710 (**1994**).
4. H. Tokuhisa, M. Zhao, A. A. Baker, V. T. Phan, D. L. Dermody, M. E. Garcia, P. F. Peez, R. M. Crooks, and T. M. Mayer, *J. Am. Chem. Soc.* 120, 4492 (**1998**).
5. M. Schlupp, T. Weil, A. J. Berresheim, U. M. Wiesler, J. Bargon, and K. Müllen, *Angew. Chem. Int. Ed.* 40, 4011 (**2001**).
6. S. Chen, Q. Yu, L. Li, C. L. Boozer, J. Homola, S. S. Yee, and S. Jiang, *J. Am. Chem. Soc.* 124, 3395 (**2002**).
7. D. Patton, M.-K. Park, S. Wang, and R. C. Advincula, *Langmuir* 18, 1688 (**2002**).
8. S.-K. Oh, L. A. Baker, and R. M. Crooks, *Langmuir* 18, 6981 (**2002**).
9. J. Won, K. J. Ihn, and Y. S. Kang, *Langmuir* 18, 8246 (**2002**).
10. H. C. Choi, W. Kim, D. Wang, and H. Dai, *J. Phys. Chem. B* 106, 12361 (**2002**).
11. H. Nagaoka and T. Imae, *Trans. Mater. Res. Soc. Jpn.* 26, 945 (**2001**).
12. H. Nagaoka and T. Imae, *International Journal of Nonlinear Sciences and Numerical Simulation* 3, 223 (**2002**).
13. M. Ito, T. Imae, K. Aoi, K. Tsutsumiuchi, H. Noda, and M. Okada, *Langmuir* 18, 9757 (**2002**).
14. M. Wells and R. M. Crooks, *J. Am. Chem. Soc.* 118, 3988 (**1996**).
15. H. Tokuhisa and R. M. Crooks, *Langmuir* 13, 5608 (**1997**).
16. D. Arrington, M. Curry, and S. C. Street, *Langmuir* 18, 7788 (**2002**).
17. H. Li, D. J. Kang, M. J. Blamire, and E. T. S. Huck, *Nano Lett.* 2, 347 (**2002**).
18. R. McKendry, W. T. S. Huck, B. Weeks, M. Fiorini, C. Abell, and T. Rayment, *Nano Lett.* 2, 713 (**2002**).
19. H. Sugimura and N. Nakagiri, *Appl. Phys. A* 66, S427 (**1998**).
20. H. Sugimura, K. Ushiyama, A. Hozumi, and O. Takai, *Langmuir* 16, 885 (**2000**).
21. L. Hong, K. Hayashi, H. Sugimura, O. Takai, N. Nakagiri, and M. Okada, *Surf. Coat. Technol.* 169, 211 (**2003**).
22. L. Hong, H. Sugimura, T. Furukawa, and O. Takai, *Langmuir* 19, 1966 (**2003**).
23. M. Osawa, *Bull. Chem. Soc. Jpn.* 70, 2861 (**1997**).
24. T. Imae, *Encyclopedia of Surface and Colloid Science* edited by M. Dekker 3547 (**2002**).
25. X. C. Wu, A. M. Bittner, and K. Kern, *Langmuir* 18, 4984 (**2002**).
26. A. M. Bittner, X. C. Wu, and K. Kern, *Adv. Funct. Mater.* 12, 432 (**2002**).
27. E. Kim, K. Kim, H. Yang, Y. T. Kim, and Kwak, *J. Anal. Chem.* 75, 5665 (**2003**).
28. H. C. Yoon, M.-Y. Hong, and H.-S. Kim, *Langmuir* 17, 1234 (**2001**).
29. M.-Y. Hong, H. C. Yoon, M.-Y. Hong, and H. S. Kim, *Langmuir* 19, 416 (**2003**).
30. C. Plank, K. Mechtler, F. C. Szoka, Jr., and E. Wagner, *Human Gene Ther.* 7, 1437 (**1996**).
31. A. U. Bielinska, J. F. Kukowska-Latallo, J. Johnson, D. A. Tomalia, and J. R. Baker, Jr., *Nucleic Acids Res.* 24, 2176 (**1996**).
32. V. A. Kabanov, A. B. Zezin, V. B. Rogacheva, Z. G. Gulyaeva, M. F. Zansochova, J. G. H. Joosten, and J. Brackman, *Macromolecules* 32, 1904 (**1999**).
33. V. A. Kabanov, V. G. Sergeyev, O. A. Pyshkina, A. A. Zinchenko, A. B. Zezin, J. G. H. Joosten, J. Brackman, and K. Yoshikawa, *Macromolecules* 33, 9587 (**2000**).
34. W. Chen, N. J. Turro, and D. A. Tomalia, *Langmuir* 16, 15 (**2000**).
35. T. Imae, T. Hirota, K. Funayama, K. Aoi, and M. Okada, *J. Colloid Interf. Sci.* 263, 306 (**2003**).
36. D. Leisner and T. Imae, *J. Phys. Chem. B* 107, 8078 (**2003**).
37. T. Imae and A. Miura, *J. Phys. Chem. B* 107, 8088 (**2003**).
38. D. Leisner and T. Imae, *J. Phys. Chem. B* 107, 13158 (**2003**).
39. D. Leisner and T. Imae, *J. Phys. Chem. B* 108, 1798 (**2004**).
40. A. Mitra and T. Imae, *Biomacromolecules* 5, 69 (**2004**).
41. K. Inoue, M. Michimori, M. Okuyama, and H. Hamakawa, *Jpn. J. Appl. Phys.* 26, 805 (**1987**).
42. A. Holländer, J. E. Klemberg-Sapieha, and M. R. Wertheimer, *Macromolecule* 27, 2893 (**1994**).
43. A. Hozumi, K. Ushiyama, H. Sugimura, and O. Takai, *Langmuir* 15, 7600 (**1999**).
44. Z. Zhang and T. Imae, *J. Colloid Interf. Sci.* 233, 99 (**2001**).
45. Z. Zhang and T. Imae, *J. Colloid Interf. Sci.* 233, 107 (**2001**).
46. H. Sugimura and N. Nakagiri, *J. Photopolym. Sci. Technol.* 10, 661 (**1997**).
47. H. Sugimura, A. Hozumi, T. Kameyama, and O. Takai, *Surf. Interf. Anal.* 34, 550 (**2002**).
48. H. Sugimura, K. Hayashi, N. Saito, L. Hong, O. Takai, A. Hozumi, N. Nakagiri, and M. Okada, *Trans. Mater. Res. Soc. Jpn.* 27, 545 (**2002**).
49. T. Yamazaki and T. Imae, *J. Nanosci. Nanotech.* 5, 1066 (**2005**).
50. I. B. Rietveld and D. Bedeaux, *Macromolecules* 33, 7912 (**2000**).
51. J. Li, L. T. Piehler, D. Qin, J. R. Baker, Jr., and D. A. Tomalia, *Langmuir* 16, 5613 (**2000**).
52. A. Wada, *J. Chem. Phys.* 29, 674 (**1958**).
53. A. Wada, *J. Chem. Phys.* 30, 328 (**1959**).

Received: 8 May 2005. Revised/Accepted: 22 July 2005.